Synthesis and Characterization of Styrene/Maleimide Copolymer with 4-[*N*-ethyl-*N*-(2-hydroxyethyl) amino]-4′-nitroazobenzene as Side Chain

Hongting Pu,[1] Ling Liu,[1] Weichun Jiang,[1] Xinwan Li,[2] Jianping Chen[2]

[1]*Institute of Functional Polymers, School of Materials Science and Engineering, Tongji University, Shanghai 200092, China*
[2]*State Key Laboratory of Local Optical Fiber Communication and Advanced Optical Communication System, Shanghai 200030, China*

Received 8 May 2006; accepted 9 March 2007
DOI 10.1002/app.27809
Published online 23 January 2008 in Wiley InterScience (www.interscience.wiley.com).

ABSTRACT: Relatively low thermal stability of second-order nonlinear optical (NLO) coefficient due to the relaxation of dipole orientation is a major problem limiting the practical application of these NLO polymers. NLO polymers with suitable T_g are always important for optical devices. In the present work a synthetic approach to styrene-(*N*-(4-hydroxyphenyl) maleimide) copolymer (SHMI) with 4-[*N*-ethyl-*N*-(2-hydroxyethyl) amino]-4′-nitroazobenzene (DR1) as side chain and chromophores has made it possible to efficiently prepare a NLO polymer. The copolymer with high T_g of 202°C has low relaxation of dipole orientation. The maximum optical loss at the optical communication wavelength is less than 0.9 dB. NLO coefficient r_{33} is 8.2 pm/V (1550 nm) and its maximum relaxation at room temperature is 18%. © 2008 Wiley Periodicals, Inc. J Appl Polym Sci 108: 1378–1384, 2008

Key words: nonlinear optical (NLO) polymer; styrene-maleimide copolymer; dispersed red; side chain; corona poling

INTRODUCTION

Organic second-order nonlinear optical (NLO) polymers offer great promise for use in high-speed electro-optical (EO) devices with broad bandwidth, low drive voltages, flexibility in fabrication and processing techniques that are compatible with integrated circuit technology.[1–7] Relatively low temporal stability of second-order NLO coefficient due to the relaxation of dipole orientation is a major problem limiting the practical application of these NLO polymers.[8] There are two main ways to suppress the relaxation. One is to introduce crosslinking structure into NLO materials.[9,10] The other is to synthesize high T_g NLO polymers having rigid backbones with chromophores as side chain.[11,12] Many efforts have been made to attain high T_g polymers.[13–16] Polyimide materials have been investigated because of their excellent NLO stability at elevated temperatures.[17–21] However, NLO polymers with high T_g are not always beneficial for optical devices. A poling process to align the optical polymer takes place efficiently around T_g under the high electric fields. Too high temperature under the electric fields may cause dielectric breakdown of the optical polymer or buffered layers, which limits using high electric fields for the efficient alignment. It is worthy to find polymers with suitable T_g for the reason.[22] It seems that the NLO-active polymers based on styrene/maleimide copolymers and 4-[*N*-ethyl-*N*-(2-hydroxyethyl) amino]-4′-nitroazobenzene (DR1), which is a frequently used chromophore,[23] can meet the basic demands of application in terms of EO coefficient, stability, optical loss, and so on.

In the present work a NLO polymer (SHMI-DR1) based on styrene/maleimide copolymer, with DR1 as side chain and chromophore, was synthesized. The synthesis begins from the preparation of *N*-(4-hydroxyphenyl) maleimide (HMI), which is from maleic anhydride and 4-amino phenol as shown in Scheme 1. HMI is then copolymerized with styrene to form styrene-(*N*-(4-hydroxyphenyl) maleimide) copolymer (SHMI), which has the reactive site. The hydrogen of the phenyl OH group of SHMI can be delocalized to some extent. It can be protonized and addition polymerized with azodicarboxylic acid diethylester (DEAD), and finally SHMI-DR1 was synthesized by a reaction similar to Mitsunobu reaction during which the DR1 were linked to the SHMI by ether bonds as shown in Scheme 2. In the reaction, OH group is eliminated from DR1, while SHMI is dehydrogenated.

Correspondence to: H. Pu. (puhongting@mail.tongji.edu.cn).

Contract grant sponsor: National Natural Science Foundation of China; contract grant number: 60377013.

EXPERIMENTAL

Materials

Styrene (99+%) (Shanghai Chemical Reagent Co., Shanghai, China) was purified by reduced pressure distillation. Maleic anhydride (99.5%) (Shanghai Chemical Reagent Co., Shanghai, China) and azodicarboxylic acid diethylester (DEAD) (40 wt % methanol solution, Aldrich, St. Louis, MO) were used without further purification. 4-[*N*-ethyl-*N*-(2-hydroxyethyl) amino]-4′-nitroazobenzene (DR-1, 95%, Aldrich), ρ-aminophenol, and 2,2′-azobisisobutyronitrile (AIBN) were purified by recrystallization before use. Tetrahydrofuran (THF) was purified by dehydration with $LiAlH_4$ followed by distillation. Dimethyl formamide (DMF), *o*-xylene, triphenylphosphine (PPh_3), and other chemical reagents were all analytical grade and used as received.

Synthesis of SHMI and SHMI-DR1

N-(4-hydroxyphenyl) maleimide (HMI) was synthesized according to the patent literature,[24] and then reacted with styrene by free radical polymerization to form SHMI. The composition, yield, and molecular weight of SHMI at different feed ratio are shown in Table I. The copolymer is nearly alternating copolymer. Styrene-maleimide copolymers (SHMI-DR1) with DR1 as side chain were synthesized by Mitsunobu reaction.[25,26] Fifty milliliter flask was purged by N_2 to remove O_2. Twenty-five milliliters of THF solution with 0.586 g SHMI (feed ratio of HMI and styrene was 1 : 1), 0.756 g DR1, and 0.746 g triphenylphosphine (PPh_3) were added under N_2 atmosphere. After complete mixing, 0.962 mL 40 wt % toluene solution of DEAD was added slowly. The reaction was maintained at room temperature for 48 h. The product was precipitated by excessive methanol after concentration by a rotary evaporator. They were then thoroughly washed with methanol until the solvent was colorless. SHMI-DR1 was then dried at 50°C for 48 h in vacuum to afford a dark red solid. Yield: 0.592 mg (44%).

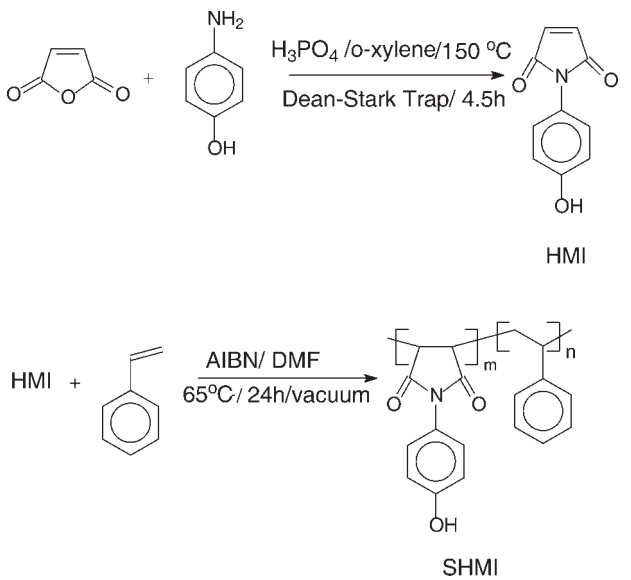

Scheme 1 Synthetic route of *N*-(4-hydroxyphenyl) maleimide (HMI) and styrene-(*N*-(4-hydroxyphenyl) maleimide) copolymer (SHMI).

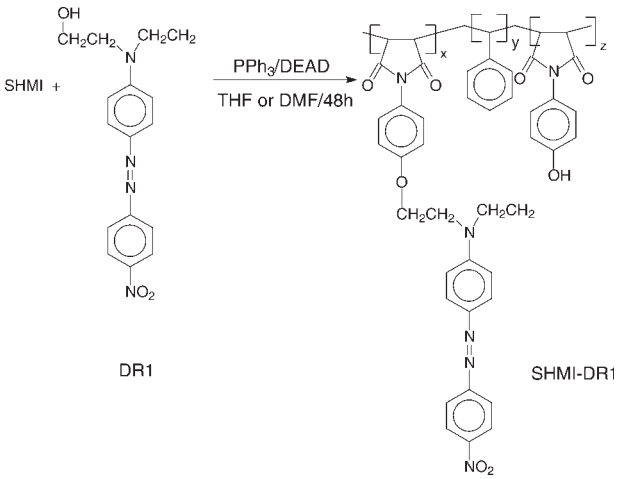

Scheme 2 Synthetic route of DR1 substituted styrene-(*N*-(4-hydroxyphenyl) maleimide) copolymer (SHMI-DR1).

Characterization of the copolymers

FTIR spectra of DR1, SHMI, and SHMI-DR1 were measured on an EQUINOX65 FTIR spectrometer. ^{1}H-NMR spectra of the copolymer were recorded on a BRUKER AVAVCE-DMX 500 spectrometer with Acetone-d6 as solvent and TMS as internal standard sample. UV–vis spectra were obtained on a HITACHI UV-250 spectrometer. Elemental analysis of the copolymer was performed on Carlo-Erba EA1110 CHNO-S analyzer. Differential scanning calorimetry (DSC) measurement was performed on a DSC-5P under N_2 atmosphere with a heating rate of 10°C/min. Thermogravimetric analysis was performed using a Perkin-Elmer TGA-7 thermogravimetric analyzer under N_2 atmosphere with a heating rate of 20°C/min. Measurement of molecular weight of the copolymers was performed using Waters 150-C gel permeation chromatography at 25°C, with THF aseluent and anion polymerized PS as standard sample.

SHMI-DR1 was deposited onto ITO Pyrex glass substrates by the spin-coating technique at 2000 rad/min from solutions of 12% of copolymers in DMF. They were dried at 80°C for 24 h. The corona poling of the films was conducted by using the poling equipment with gratings. The corona poling was performed under N_2 atmosphere at 6.5 KV using a sharp tungsten needle as electrode, which was placed 1.0 cm above the film surface at 195°C for

TABLE I
Composition, Yield, Molecular Weight, and Molecular Weight Distribution of SHMI with Different Feed Ratio

Feed ratio (HMI : St)	Repeat unit composition of the copolymers (HMI : St)[a]	Yield of copolymerization (%)	M_n ($\times 10^4$)[b]	M_w ($\times 10^4$)[b]	$d = M_w/M_n$[b]
60 : 40	48 : 52	32	2.3	5.9	2.6
50 : 50	47 : 53	92	1.6	3.8	2.3
40 : 60	45 : 55	74	1.5	2.7	2.0
33 : 67	41 : 59	52	1.2	2.2	1.8

[a] Measured by NMR and elemental analysis.
[b] Measured by GPC, THF as solvent, PS as reference.

20 min. This optimization condition is found out by calculating the order parameter of film under various poling conditions, which is defined as the ratio of decrease of absorbance to the initial absorbance. It is better if the ratio is close to 1. The change of UV–vis absorption spectra acquired from pristine NLO film and the poled film is shown in Figure 1. The morphology of pristine NLO film and the poled film was observed by metallographic microscope. Optical loss (L_o) and r_{33} of poled SHMI-DR1 film was measured by Mach-Zehnder technique.[27]

RESULTS AND DISCUSSION

Chemical structure of the copolymers

FTIR spectra of HMI and SHMI (molar ratio is 1 : 1) synthesized are shown in Figure 2. HMI and SHMI have absorption peaks at 1775 and 1705 cm^{-1}, which are the feature absorption of carbonyl group in imide. The shared absorption for both SHMI and HMI at 3100, 1600, 1520, 830 cm^{-1} is attributed to the phenyl rings and the *para*-substituted phenyl rings. HMI has an intense absorption band approximately centered at 3500 cm^{-1} due to the phenyl OH group, while SHMI has a broad band in the region of 3100–3700 cm^{-1}. The absorption peak at 1220 cm^{-1} assigned to C—O in HMI shifts down to 1194 cm^{-1} in SHMI. The absorption peaks at 760 cm^{-1} (due to the monosubstituted phenyl rings in styrene moieties) and 2928 cm^{-1} (the feature absorption of carbon chain polymer, due to the long chain of C—C) appear in spectrum for SHMI.

^{1}H-NMR spectrum of SHMI is demonstrated in Figure 3. The sharp peaks approximately at 2 and 3 ppm are assigned to the aliphatic hydrogen linked to the C—C backbone. The aromatic hydrogen in the phenyl rings are indicated by the two medium and broad peaks centered at 6.8 and 7.2 ppm, respectively. The peak at 8.6 ppm is attributed to the hydrogen in OH groups. The ratio of integration for hydrogen in phenyl rings and OH groups is about 1 : 9. From a qualitative point of view, the spectrum is consistent with the polymer structure.

Figure 4 is the FTIR spectra of SHMI-DR1, SHMI, and DR1. Compared with SHMI, SHMI-DR1 has a

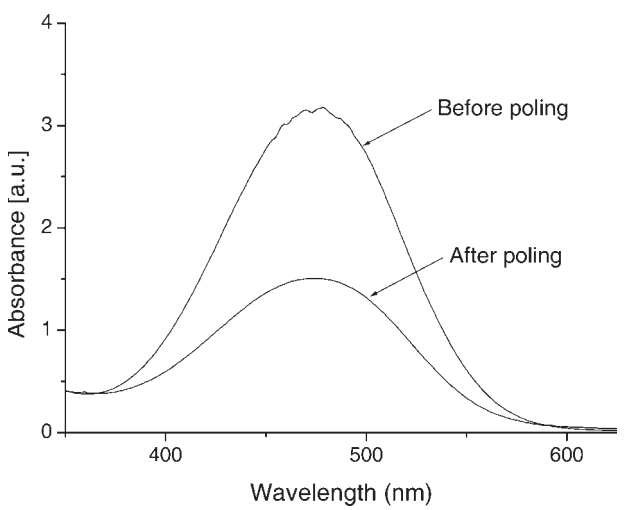

Figure 1 The change of UV–vis absorption spectra acquired from pristine NLO film and the poled film.

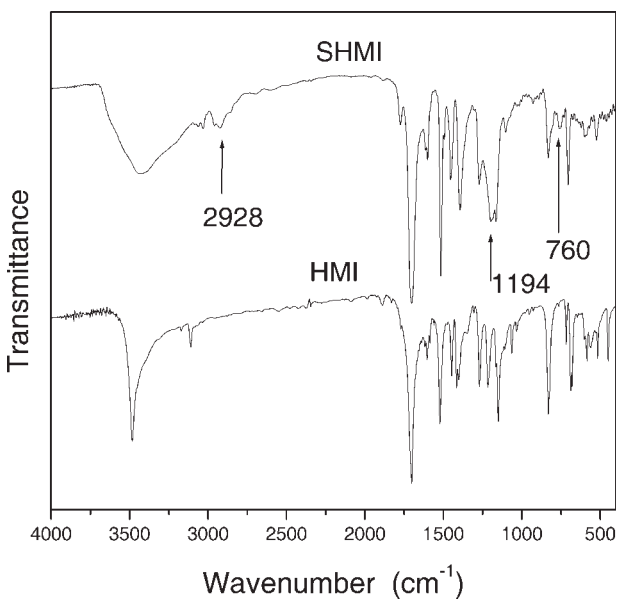

Figure 2 FTIR spectra of *N*-(4-hydroxyphenyl) maleimide (HMI) and styrene/*N*-(4-hydroxyphenyl) maleimide (1 : 1) copolymer (SHMI).

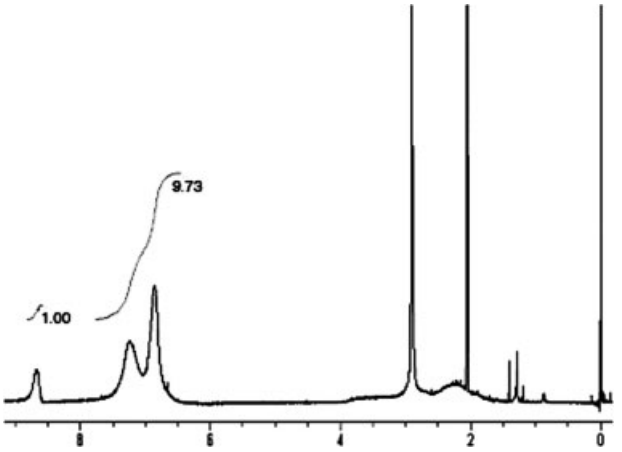

Figure 3 ^{1}H-NMR spectrum of styrene/*N*-(4-hydroxyphenyl) maleimide (1/1) copolymer (SHMI).

medium intense absorption band at 1340 cm^{-1}, which is the feature absorption of nitro group in DR1. Absorption at 1600 cm^{-1} and in the region of 700–800 cm^{-1} of SHMI-DR1 is much more intense than SHMI due to the increased concentration of phenyl rings introduced by DR1.

^{1}H-NMR spectrum of SHMI-DR1 is demonstrated in Figure 5. Compared with that for SHMI, two weak peaks are observed in spectrum for SHMI-DR1 in the 8.0–8.5 ppm due to hydrogen in phenyl rings linked to NO_2 group in DR1 and hydrogen in azobenzene. SHMI-DR1 has OH groups that have not been substituted. Comparing SHMI with SHMI-DR1, chemical shift of the phenyl OH group shifts from 8.6 to 9.6 ppm. This is attributed to the hydrogen bond formed between NO_2 group in DR1 and phenyl OH group. The peaks at 6.2–7.8 ppm are attributed to the aromatic hydrogen. The sharp peaks at

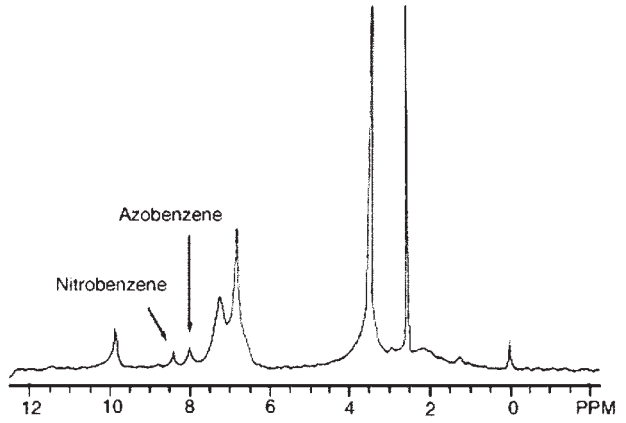

Figure 5 ^{1}H-NMR spectra of SHMI-DR1.

2–4 ppm are attributed to the hydrogen of —CH_2—, —CH—, and —CH_3 in DR1.

UV–vis spectra of SHMI-DR1 and substitution ratio of DR1

UV–vis spectra of THF solution of SHMI-DR1 and DR1 are shown in Figure 6. The maximum absorption wavelengths (λ_{max}) of SHMI-DR1 and DR1 are 473 and 484 nm, respectively. The π-π* transition of azobenzene in the polymer is hypsochromically shifted by 11 nm, which indicates the influence of backbone. The hindrance of backbone contributes to the increase of energy needed for π-π* transition.

The concentration of DR1 in SHMI-DR1 was estimated by UV spectrometry. Figure 6 shows the UV spectra of DR1 and SHMI-DR1. The chromophore concentration and substitution ratio of the phenyl OH groups in SHMI are obtained according to the standard curve of DR1 (as shown in Fig. 7). The

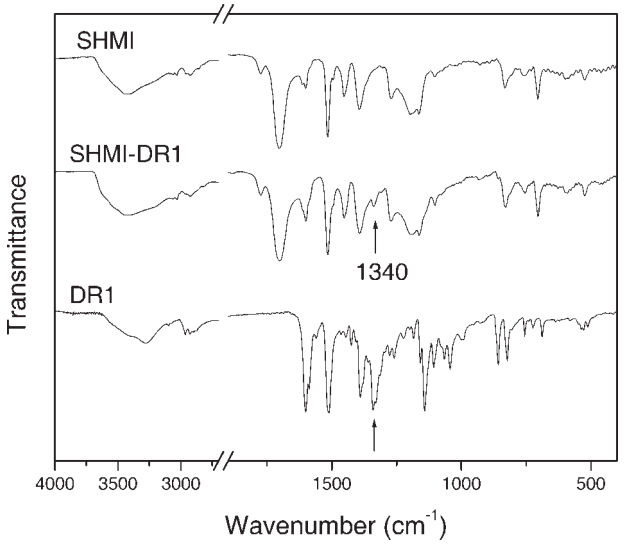

Figure 4 FTIR spectra of SHMI-DR1, SHMI, and DR1.

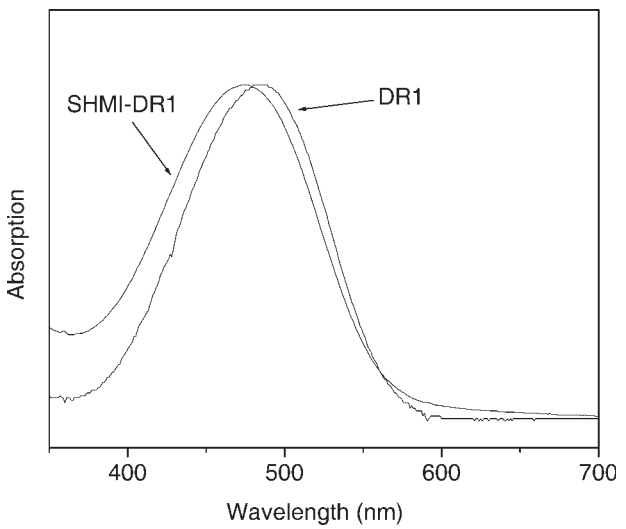

Figure 6 UV–vis spectra of DR1 and SHMI-DR1 (in THF solution).

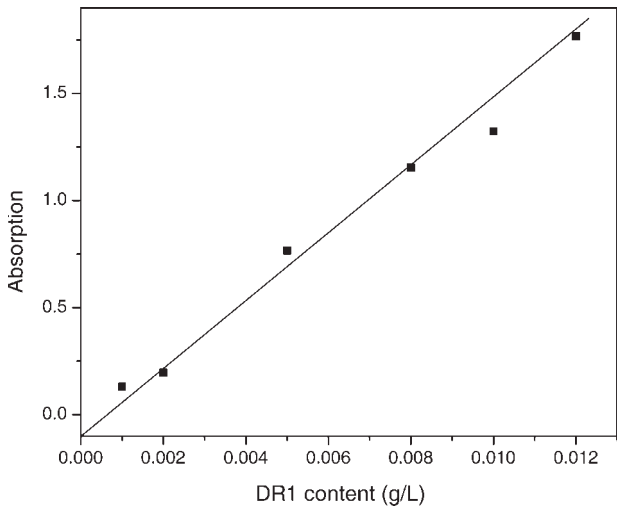

Figure 7 Standard curve of DR1 in THF solution.

chromophore concentration in SHMI-DR1 and the substitution ratio were calculated to be 12 wt % and 13%, respectively.

GPC results of SHMI and SHMI-DR1 are shown in Table II. It is indicated that SHMI-DR1 has a slightly larger molecular weight due to the side-chain chromophore. The substitution ratio of DR1 can be calculated from the change in M_n caused by the introduction of DR1. Suppose the mass concentration of DR1 is W_D%, the number average mass before and after substitution are M_1 and M_2, respectively. Thus W_D% can be calculated by the relation,

$$W_D\% = \frac{M_2 - M_1}{M_2} \times 100\% \quad (1)$$

The results almost consist with the results of UV–vis spectra.

Table II also lists the elemental analysis results of SHMI-DR1. The theoretical values are calculated on the assumption that the content of DR1 moieties of SHMI-DR1 is 12 wt %. It is observed that the elemental analysis results are in accordance with the

TABLE II
Molecular Weight of SHMI-DR1 and Substitution Ratio of DR1 in SHMI-DR1

	M_n[a] ($\times 10^4$)	M_w[a] ($\times 10^4$)	$d = M_n/M_w$[a]	Theoretical values C (wt %)	Theoretical values H (wt %)	Practical values[b] C (wt %)	Practical values[b] H (wt %)
SHMI	1.65	3.85	2.33	73.72	5.12	73.05	5.16
SHMI-DR1	1.84	4.44	2.41	72.71	5.09	72.54	5.12

[a] Measured by GPC, THF as solvent, PS as reference.
[b] Measured by elemental analysis.

TABLE III
Solubility of SHMI-DR1

Acetone	+
THF	+
DMF	+
Chloroform	+/−
Ethyl acetate	−
Cyclohexane	−
Ethylene diamine	−
Acetic anhydride	−
Toluene	+/−
o-xylene	+/−
Dimethyl sulfoxide	+
Styrene	−

+, soluble; +/−: partially soluble; −: insoluble.

structure of copolymers. The structure of SHMI-DR1 is confirmed by the above results.

Solubility of SHMI-DR1

The solubility of SHMI-DR1 in different solvents is listed in Table III. It is indicated that SHMI-DR1 has better solubility in solvents, which can form H-bonding with its phenyl OH groups that are not substituted. Because of the DR1 group, SHMI-DR1 is slightly soluble in hydrophobic solvents such as chloroform and *o*-dichlorobenzene. SHMI-DR1 has good solubility in the solvents with low boiling points such as acetone and THF. This provides SHMI-DR1 with good film-forming ability by spin-coating technique.

Thermal properties of SHMI-DR1

T_g of SHMI-DR1 obtained from DSC thermogram is about 202°C which is little lower than that of SHMI (253°C), but much higher than many side-chain NLO

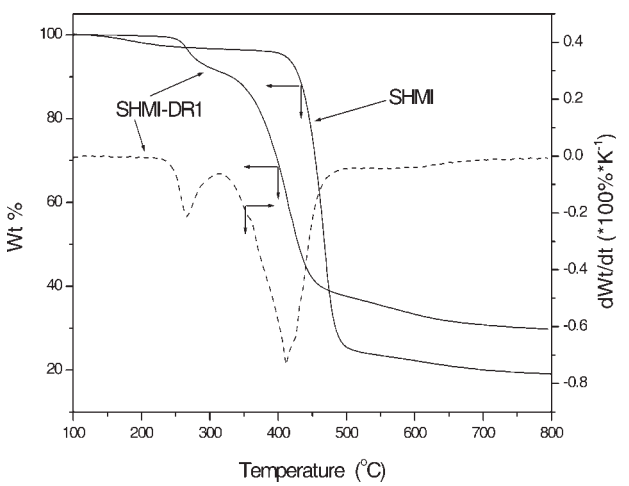

Figure 8 TGA and DTG analysis of SHMI-DR1.

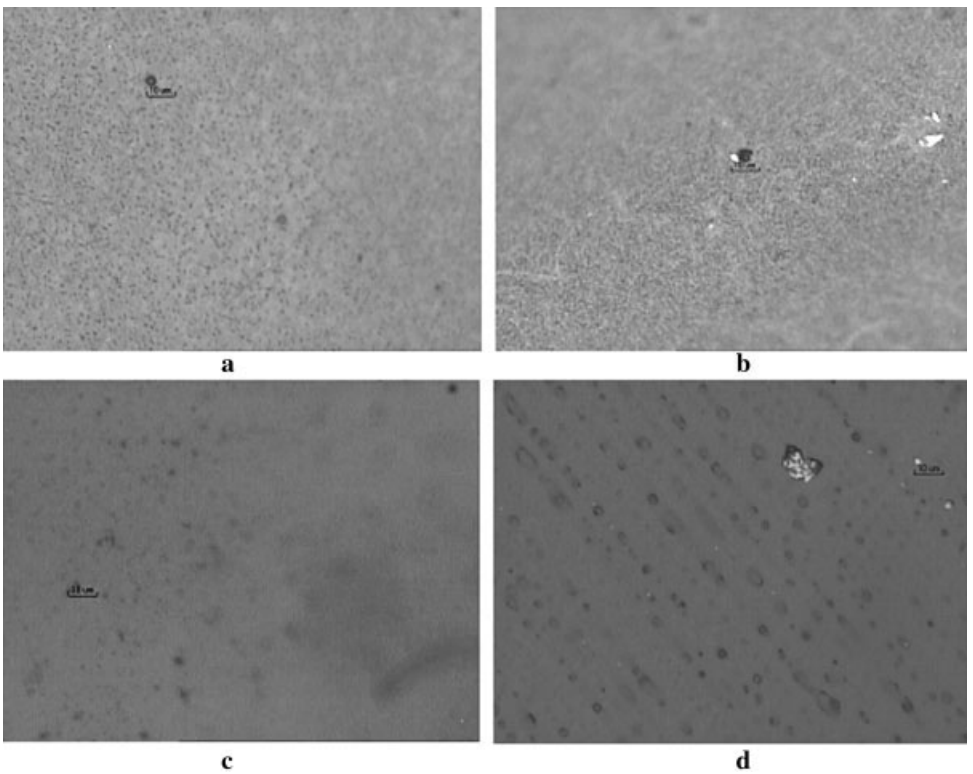

Figure 9 Morphology of pristine DR1 doped SHMI film (a), poled DR1 doped SHMI film (b), pristine SHMI-DR1 film (c), and poled SHMI-DR1 film (d) observed by metallographic microscope.

polymers.[28] TGA and DTG analysis of SHMI-DR1 are displayed in Figure 8. SHMI-DR1 begins to degrade at 244°C. The thermal stability of SHMI-DR1 is worse than that of SHMI but better than DR1 whose degradation temperature is ~ 220°C.[29] The degradation process can be divided into three phases. The weight loss at T_{d2} (324°C) is 11%, which is close to the concentration of DR1. It can be concluded that the first phase in the degradation process (T_{d1} and T_{d2}) should be attributed to the thermal degradation of DR1 groups. The curve in the second phase is very similar to that of SHMI. This phase consists of the breakdown of backbones and the decomposition of phenyl rings. In the second phase, SHMI-DR1 initially degrades and maximally degrade at lower temperatures than those of SHMI due to the decrease of molecular regularity of SHMI-DR1 and the destruction of hydrogen bond. But SHMI-DR1's T_{d1} is 40°C higher than its T_g and is thermally stable enough to be applied in EO devices.

The morphology of SHMI-DR1 films

Figure 9 shows the morphology of pristine NLO film and the poled film observed by metallographic microscope. No significant difference was observed between the morphology of pristine DR1 doped SHMI film and the poled film. It can also be found that the morphology of pristine SHMI-DR1 film was homogeneous. Club-shaped structures in the poled film indicate the orientation of SHMI-DR1 in bulk, which is induced under the electric field.

Linear and nonlinear optical properties

The optical loss (L_o) of SHMI-DR1 films at the optical communication wavelength is displayed in Figure 10. It is observed that the maximum optical loss of

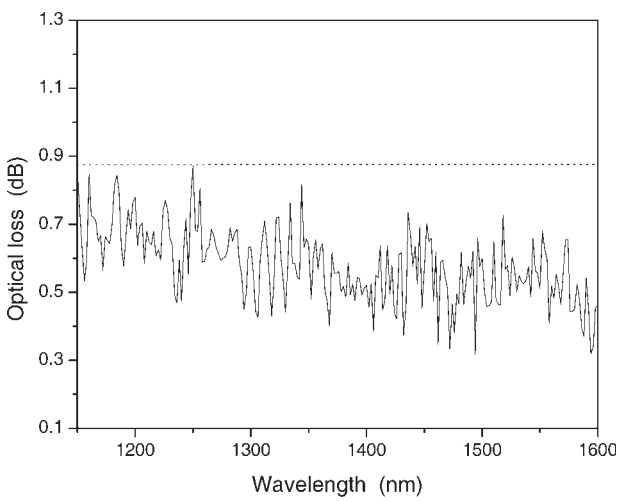

Figure 10 Optical loss of SHMI-DR1 in the range of optic communication wavelength.

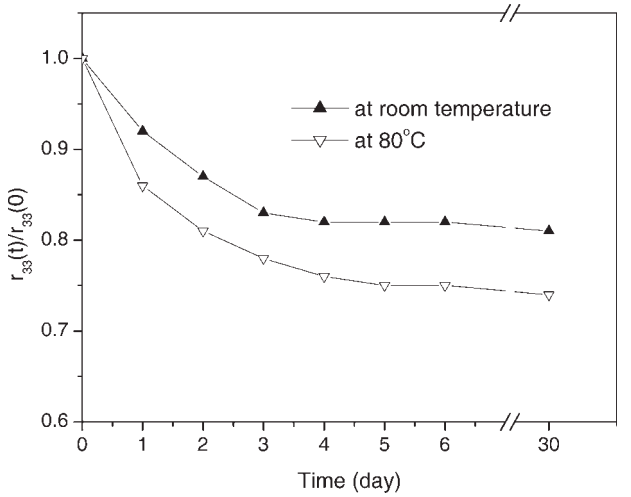

Figure 11 Curves of r_{33} relaxation with time at room temperature and 80°C, respectively.

SHMI-DR1 at the communication wavelength is 0.89 dB (1250 nm) and the optical loss at most wavelengths is less than 0.75 dB. Especially at some particular wavelengths, at which r_{33} is usually detected, L_o are 0.87 dB (1180 nm), 0.58 dB (1300 nm), 0.42 dB (1310 nm), and 0.71 dB (1550 nm), respectively. All these indicate that SHMI-DR1 film meets the demands of device application as for optical loss.

r_{33} of poled SHMI-DR1 film detected by Mach-Zehnder technique[27] is 8.2 pm/V (1550 nm). Its r_{33} at shorter wavelength (e.g. 1300, 1180, 632.8 nm, etc) may be higher. Figure 11 shows the stability of r_{33}. It gives the values of r_{33} at different temperatures as a function of time. Figure 11 indicates that the electro-optic coefficient of side-chain SHMI-DR1 loses 18 and 22% at room temperature and 80°C, respectively, and then maintains constant. The reason is that in the side-chain poled polymers the chromophores are linked to the main chains of the copolymers by chemical bonds, which can reduce orientation relaxation. SHMI-DR1 meets the basic demands of device application as for the electro-optic coefficient and the stability of the electro-optic effect.

CONCLUSIONS

NLO polymer based on *N*-(4-hydroxyphenyl) maleimide-*alt*-styrene copolymer with DR1 as side chain was synthesized by Mitsunobu substitution reaction. The synthesized copolymer has good solubility and an appropriate T_g of 202°C, which gets a balance between the low relaxation and low possibility for dielectric breakdown. When DR1 content in the copolymer is about 11 wt %, r_{33} of SHMI-DR1 is 8.2 pm/V (at 1550 nm) and the maximum loss at room temperature is 18%. The maximum optical loss at the optical communication wavelength is less than 0.9 dB. It can be concluded that SHMI-DR1 synthesized is a promising NLO polymer for optical device.

References

1. Shi, Y.; Zhang, C.; Zhang, H.; Bechtel, J. H.; Dalton, L. R.; Robinson, B. H.; Steier, W. H. Science 2000, 288, 119.
2. Lee, M.; Katz, H. E.; Erben, C.; Gill, D. M.; Gopalan, P.; Heber, J. D.; McGee, D. J. Science 2002, 298, 1401.
3. Coe, B. J.; Jones, L. A.; Harris, J. A.; Brunschwig, B. S.; Asselberghs, I.; Clays, K.; Persoons, A. J Am Chem Soc 2003, 125, 862.
4. Verbiest, T.; Elshocht, S. V.; Karuanen, M.; Heliemans, L.; Snauwaert, J.; Nuckolls, C.; Katz, T. J.; Persoons, A. Science 1998, 282, 913.
5. Marder, S. R.; Kippelen, B.; Jen, A. K. Y.; Peyghambarian, N. Nature 1997, 388, 845.
6. Zhu, P.; Van der Boom, M. E.; Kang, H.; Evmenenko, G.; Dutta, P.; Marks, T. J Chem Mater 2002, 14, 4982.
7. Van der Boom, M. E. Angew Chem Int Ed 2002, 41, 3363.
8. Kajzar, F.; Lee, K. S.; Jen, K. Y. Adv Polym Sci 2003, 161, 1.
9. Kowalczyk, T. C.; Kosc, T. Z.; Singer, K. D.; Beuhler, A. J.; Wargowski, D. A.; Cahill, P. A.; Seager, C. H.; Meinhardt, M. B. J Appl Phys 1995, 78, 5876.
10. Luo, J. D.; Haller, M.; Li, H. X.; Kim, T. D.; Jen, K. Y. Adv Mater 2003, 15, 1635.
11. Verbiest, T.; Burland, D. M.; Jurich, M. C.; Lee, V. Y.; Miller, R. D.; Volksen, W. Science 1995, 268, 1604.
12. Man, H. T.; Yoon, H. N. Appl Phys Lett 1998, 72, 540.
13. Lee, H. J.; Lee, M. H.; Han, S. G.; Kim, H. Y.; Ahn, J. H.; Lee, E. M.; Won, Y. H. J Polym Sci Part A: Polym Chem 1998, 36, 301.
14. Samyn, C.; Ballet, W.; Verbiest, T.; Van Beylen, M.; Persoons, A. Polymer 2001, 42, 8511.
15. Saadeh, H.; Gharavi, A.; Yu, D.; Yu, L. Macromolecules 1997, 30, 5403.
16. Jen, K. Y.; Wu, X.; Ma, H. Chem Mater 1998, 10, 471.
17. Leng, W. N.; Zhou, Y. M.; Xu, Q. H.; Liu, J. Z. Polymer 2001, 42, 9253.
18. Tang, H.; Cao, G.; Taboada, J. M.; Chen, R. T. J Polym Sci Part B: Polym Phys 1997, 35, 2385.
19. Jeng, R. J.; Chang, C. C.; Chen, C. P.; Chen, C. T.; Su, W. C. Polymer 2003, 44, 143.
20. Jeng, R. J.; Hung, W. Y.; Chen, C. P.; Hsiue, G. H. Polym Adv Technol 2003, 14, 66.
21. Lu, J.; Yin, J. J Polym Sci Part A: Polym Chem 2003, 41, 303.
22. Do, J. Y.; Park, S. K.; Ju, J. J.; Park, S.; Lee, M. H. Opt Mater 2004, 26, 223.
23. Toussaere, E.; Labbe, P. Opt Mater 1999, 12, 357.
24. Nippon Shokubai Co. JP 0,319,226 (1991).
25. Mitsunobu, O. Synthesis 1981, 1, 1.
26. Mitsunobu, O.; Takizawa, S.; Morimoto, H. J Am Chem Soc 1969, 91, 6510.
27. Ma, C. B.; Ren, Q. J Optoelectron Laser 1999, 10, 183.
28. Cao, X.; McHale, J. L. J Phys Chem 1997, 101, 8843.
29. Galvan-Gonzalez, A.; Canva, M.; Stegeman, G. I.; Twieg, R.; Kowalczyk, T. C.; Lackritz, H. S. Opt Lett 1999, 24, 1741.